Polymer slab waveguides for the optical detection of nanoparticles in evanescent field based biosensors

Polymer slab waveguides for the optical detection of nanoparticles in evanescent field based biosensors

Nuria Teigell Beneitez[1], Jeroen Missinne[1], Jean Schleipen[2], Joke Orsel[2], Menno W.J. Prins[2], Geert Van Steenberge[1]
[1]Centre for Microsystems Technology (CMST), imec and Ghent University, Gent, Belgium
[2]Philips Research, Eindhoven, The Netherlands

ABSTRACT

We present a polymer optical waveguide integration technology for the detection of nanoparticles in an evanescent field based biosensor. In the proposed biosensor concept, super-paramagnetic nanoparticles are used as optical contrast labels. The nanoparticles capture target molecules from a sample fluid and bind to the sensor surface with biological specificity. The surface-bound nanoparticles are then detected using frustration of an evanescent field. In the current paper we elaborate on the polymer waveguides which are used to generate a well-defined optical field for nanoparticle detection.

Keywords: biosensor, evanescent field, nanoparticle detection, polymer waveguide.

1 INTRODUCTION

The aging population and increases in chronic diseases put high pressure on the healthcare system, which drives a need for easy to use and cost-effective medical technologies. In-vitro diagnostics (IVD) plays a large role in delivering healthcare and within the IVD market, decentralized diagnostic testing, i.e. point-of-care testing (POCT), is a growing segment. Applications for which POCT is very relevant are for example the detection of protein markers to diagnose cardiac diseases and the detection of nucleic acid markers in case of infectious diseases. POCT devices should be compact and fully integrated for maximum ease of use. A new class of POCT devices is based on the use of magnetic nanoparticles[1]. Using magnetic nanoparticles has important advantages: they have a large surface-to-volume ratio, are conveniently biofunctionalized, provide a large optical contrast, and they can be manipulated by magnetic fields for full control of the integrated biosensing assay.

Here, we study a polymer optical waveguide integration technology for the detection of magnetic nanoparticles. In this biosensor concept, super-paramagnetic nanoparticles are used as optical contrast labels. The nanoparticles capture target molecules from a sample fluid and bind to the sensor surface with biological specificity. Thereafter, the surface-bound nanoparticles are detected using frustration of an evanescent field. The evanescent field is generated by total internal reflection (TIR) of light at a boundary between two media with different refractive index (RI). Evanescent field detection has been used in several biosensing concepts, such as SPR-based, fluorescence-based and interferometer-based biosensors[2,3,4], using out-of-plane as well as in-plane optical approaches. The use of in-plane waveguide methods, where the evanescent field is generated at the core-cladding interface, is interesting because this configuration is compatible with planar and therefore very compact device formats. Furthermore, the use of polymers to fabricate such waveguides is compatible with cost-effective mass production methods.

2 WAVEGUIDE DESIGN

When designing a waveguide, it is necessary to consider parameters such as the penetration depth, the uniformity of the evanescent field and the waveguide quality, which will influence the signal-to-noise ratio of the final particle detection system. Furthermore, as we need to implement a large detection area (typical dimensions 1 x 1 mm^2), two approaches have been considered, namely rectangular waveguides and slab waveguides.

A first important parameter is the penetration depth of the evanescent field at the core-cladding interface. The penetration depth is the distance in which the electric field intensity decays with 1/e of its value at the core-cladding interface. The penetration depth (P_d) of a mode in the upper cladding of a slab waveguide can be calculated with the expression:

Nanoscale Imaging, Sensing, and Actuation for Biomedical Applications XI, edited by Alexander N. Cartwright, Dan V. Nicolau, Proc. of SPIE Vol. 8954, 89540Q · © 2014 SPIE · CCC code: 1605-7422/14/$18 · doi: 10.1117/12.2036072

$$P_d = \frac{\lambda_0}{2\pi\sqrt{n_{eff}^2 - n_{cladd}^2}}$$

with λ_0 the vacuum wavelength of the light propagating in the waveguide, and n_{cladd} and n_{eff} the refractive index of the cladding material and the effective refractive index of the propagating mode, respectively. The formula shows that the penetration depth is determined by the index contrast between the effective refractive index of the mode and the cladding refractive index for each wavelength. The effective refractive index of a guided mode has a value between the highest of both cladding refractive indices, and the core refractive index.

The proposed design, sketched in Figure 1, consists of a waveguide divided into two main parts, namely the propagation and the detection region. In the detection region, the core is in direct contact with the assay fluid which is serving as upper cladding, thereby exposing the assay fluid to the waveguide evanescent field allowing particle detection. In biosensor applications, the upper cladding in the sensing area will be water-based, therefore having a refractive index close to 1.33. The refractive indices for typical polymer waveguide materials are 1.5-1.6, resulting in penetration depths of around 100-200 nm for the first mode and wavelengths between 630 and 850 nm.

A second important parameter is the uniformity of the field. Several transverse modes are allowed in rectangular waveguides. The wider the waveguide, the greater is the number of permitted modes. The presence of these higher order modes results in non-uniformity in the field in terms of its distribution on the core surface due to the successive minima and maxima along the waveguide width. This non-uniformity will generate dark areas where the nanoparticles cannot be detected. Therefore, in rectangular waveguides the quasi-uniform first mode must be selected.

Contrarily, in slab waveguides the light is only confined in one direction, hence multimode behavior is only allowed in that direction and it is possible to achieve uniformity in intensity along a wide surface. To implement a slab waveguide, the diverging mode in the waveguide should not reach the boundaries of the waveguide. This means that the slab waveguide needs to be wider than the detection region; the concrete dimensions depend on the incoupling conditions that determine the divergence of the path, see Figure 1.

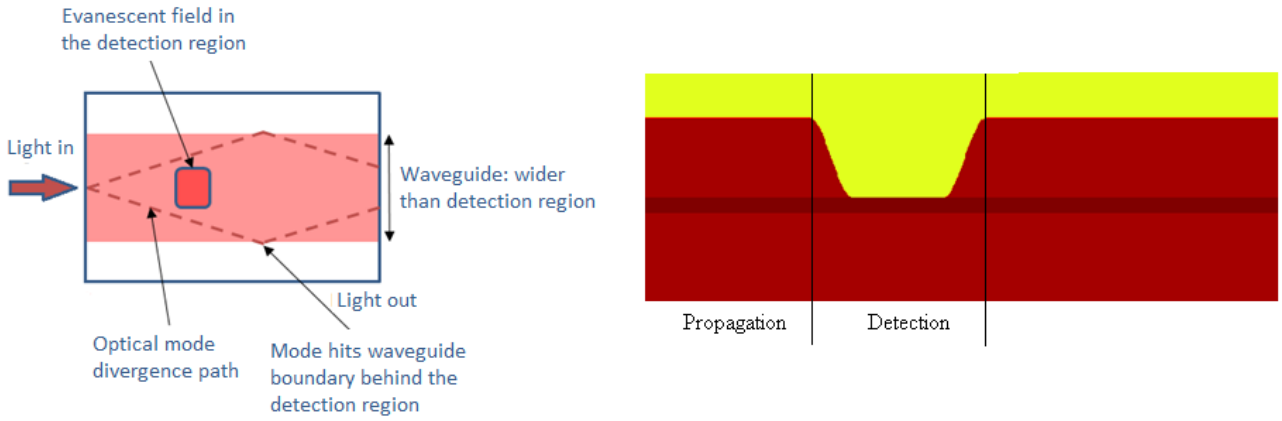

Figure 1. Schematic of a realistic slab waveguide with the detection region where nanoparticles will be detected: (left) top view, and (right) cross-section along the waveguide.

The evanescent field is also mode-dependent. The control of the light distribution along the height direction in the waveguide cross-section can be achieved by choosing the core thickness small enough so that only one mode is allowed. In a symmetric slab waveguide with core thickness d, only the fundamental TE or TM mode is allowed if:

$$d < \frac{\lambda_0}{2\sqrt{n_{core}^2 - n_{cladd}^2}}$$

In the asymmetric case, TE and TM modes are not degenerated, but if we ignore the polarization, the single mode cut-off condition for asymmetric slab waveguides can be expressed as:

$$d = \frac{\lambda_0}{2\sqrt{n_{core}^2 - n_{cladd}^2}}\left(1 + \frac{1}{\pi}\tan^{-1}\sqrt{\frac{n_{undercladd}^2 - n_{upperladd}^2}{n_{core}^2 - n_{undercladd}^2}}\right)$$

As the cut-off condition for symmetric waveguides (propagation region) is more restrictive than in the asymmetric case (detection region), the symmetric waveguide was designed to be single mode, such that also the asymmetric waveguide will be single mode.

For rectangular waveguides, no analytical solution exists and the use of FDTD simulations is convenient to obtain the propagating field parameters[5]. The thickness for which single mode behavior is obtained is slightly larger than in the case of a slab waveguide.

In the following, a general analysis is presented regarding the influence of the waveguide parameters on the penetration depth of the evanescent field, which is used to determine the waveguide designs. Although the analysis was performed for slab waveguides, the qualitative results are also valid for rectangular waveguides.

Figure 2 plots the penetration depth of the first mode in the upper cladding (i.e. water, RI 1.33) as a function of core refractive index for different combinations of wavelength and refractive index contrast (RIC) of the core and under cladding in a slab waveguide. The refractive index of the core clearly has the largest influence on the penetration depth. The closer this index is to the index of the analyte (water, refractive index 1.33), the higher the penetration depth of the evanescent field.

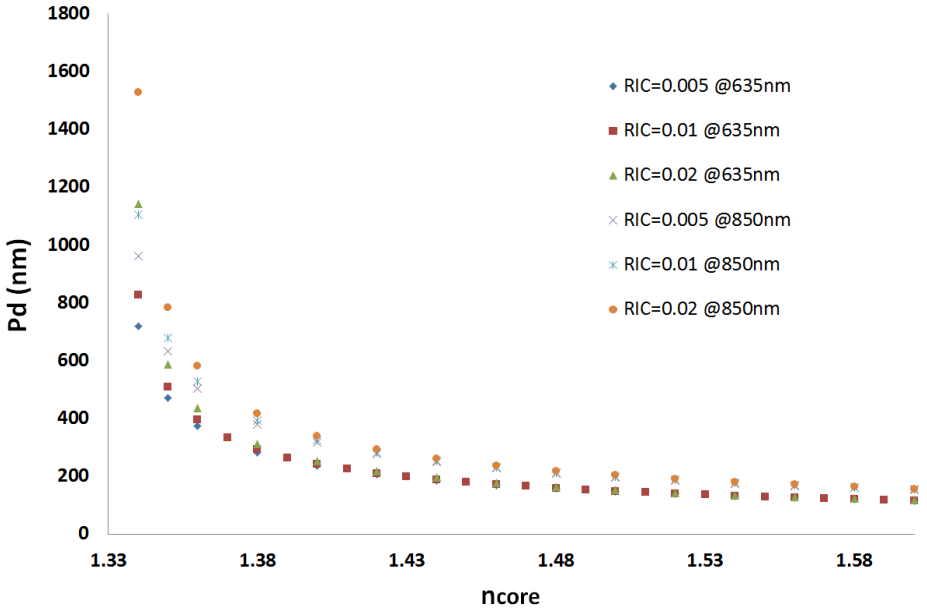

Figure 2. First mode penetration depth P_d of the waveguide evanescent field in the upper cladding (water) for different core refractive indices and core under cladding RI contrast values at 635 nm and 850 nm in a slab waveguide. The core thickness was chosen close to the single mode thickness cut-off value of the symmetric waveguide section.

The penetration depth is also influenced by the RIC between the core and under cladding, by the wavelength and by the core thickness. However, these influences are mainly appreciable when low refractive index materials are used for the core. On the other hand, the wavelength and the RIC have a strong influence on the intrinsic scattering of the waveguides[6], and on the single mode thickness condition.

After considering the above mentioned waveguide parameters, simulations on rectangular waveguide designs were performed using FDTD Solutions from Lumerical. With this software it is possible to obtain the waveguide mode field

profiles and their effective refractive indices. We simulated the mode profiles for different structures and dimensions in order to determine their single mode conditions. To check the validity of these results, the light distribution was measured experimentally. FDTD simulations can also be used to obtain the penetration depth through the analysis of the simulated intensity profiles.

3 FABRICATION

The fabrication of slab waveguides made from Ormocer polymer is described in the following. First of all, 5 x 5 cm^2 Borofloat glass substrates are cleaned by successive rinsing steps in acetone, in a mix of acetone & IPA and in DI water (2 minutes in each bath) and dried for 15 minutes on a hotplate at 150°C. Next, a surface plasma treatment cleaning step is performed in order to improve the adhesion between glass and polymer. Just after the treatment, the Ormocer under cladding layer is deposited by means of spin-coating at 3000 rpm for one minute, followed by a prebake at 80ºC on a hotplate for 5 minutes. The cladding layer is then UV-cured by flood exposure for 30 seconds at a power density of 8.6 mW/cm^2 and post exposure baked for 5 minutes at 80°C. The layer needs to be developed in OrmoDev for 3 seconds to remove the non-cured layer of the Ormocer. The developed polymer is then rinsed in IPA two times and dried with a nitrogen gun.

A hard-bake step is applied for 90 minutes at 150°C in a convection oven. The core layer is processed following the same steps but with the core version of the Ormocer polymer. The layer is spin-coated at 6000 rpm for 2 minutes to achieve a thickness below the single-mode-condition, calculated to be 1.5 µm at 635 nm for slab waveguides with refractive indices 1.538 (cladding) and 1.553 (core).

The upper cladding is processed with the same parameters as the under cladding but using a mask to define the reaction chamber. As the material is not hard after the first hot plate step, the mask cannot be in contact with the layer and thus the illumination must be performed in proximity. The developing time for the reaction chamber is 1 minute. Rectangular waveguides were fabricated with the same process but using a lithography mask to define the core pattern and developing for one minute.

Using similar parameters, LightLink and mr-LDW waveguides were fabricated. Figure 3 shows cross-sections of example rectangular and slab waveguides fabricated.

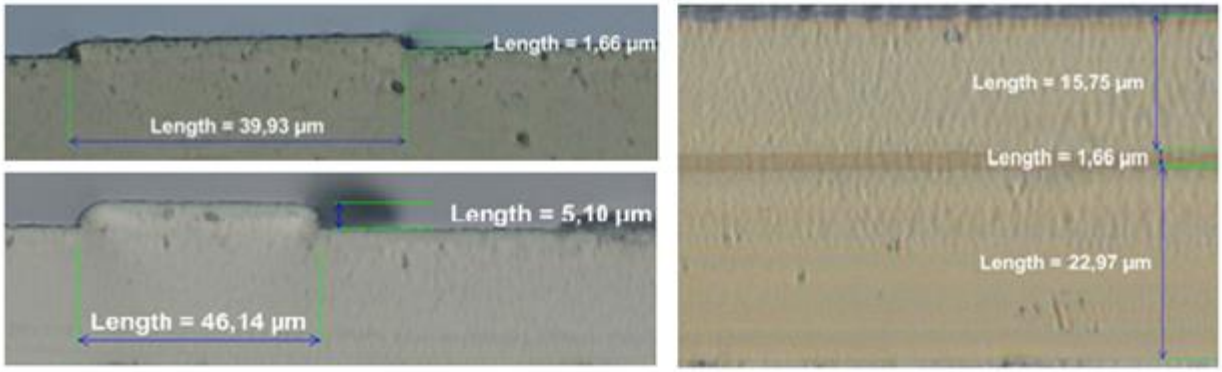

Figure 3. Cross-section of rectangular waveguides with 2 different thicknesses and not covered by upper cladding (left), and a slab waveguide covered by upper cladding (right).

4 RESULTS

4.1 Waveguide characterization

The optical quality of the polymer layers (Ormocer, LightLink and mr-LDW) was characterized in terms of roughness using a Wyko® NT3300 optical profiler, where the considered parameter was the standard deviation of the profile heights, after removing large-scale tilt and curvature effects of the surface. The data presented in this paper corresponds to ~1 mm^2 surfaces measured at random positions over the complete sample. Roughness measurements showing fabrication defects were excluded from analysis because they do not represent the intrinsic roughness of the material. The results indicate that the roughness for Ormocer and LightLink (cladding and core versions) is about 2-4 nm and the

roughness of the epoxy photopolymer, mr-LDW, was around 1 nm. Since the measured layer roughness is rather low, it is expected that this will only lead to a small amount of parasitic background scattering in the waveguide, being much smaller than the signal generated by the nanoparticles themselves.

To characterize the profile of the light in the waveguides, a commercial camera-based Near-Field Beam Profiler was used. A CCD camera, Near-Field adapter and microscope objective were acquired from Ophir Optronics. First, samples were diced with a diamond blade in order to make clean cross-sections. Next, light was coupled into the waveguides with a tapered fiber and the out-coupled light was focused with a 40x objective onto a CCD camera. The beam imaging and data recording was performed using BeamGage® software (Ophir Optronics).

Varying the incoupling parameters, it was possible to excite different modes of the waveguide. When no variation in the light profile over de waveguide cross-section was found, it was considered single mode. This was furthermore compared with the calculations of the single mode conditions, based on waveguide layer thickness and refractive index data.

Figure 4 illustrates the different intensity distributions of the light in cross-sections of a rectangular and slab waveguide, respectively. Despite the fact that the quasi-uniform first mode is theoretically allowed in the rectangular waveguide, it was found experimentally that higher order modes were almost always displayed, being strongly dependent on small changes in the incoupling parameters. The presence of these lateral higher order modes gives rise to differences in the illumination intensities of nanoparticles located at different positions in the detection region. In the case of the slab waveguide, these differences are substantially smaller, as is shown in the figure. The intensity variation in the slab waveguide mode profile includes a contribution from the noise caused by the roughness of the waveguide end-face due to dicing and therefore the actual uniformity of the field is expected to be better than shown in Figure 4.

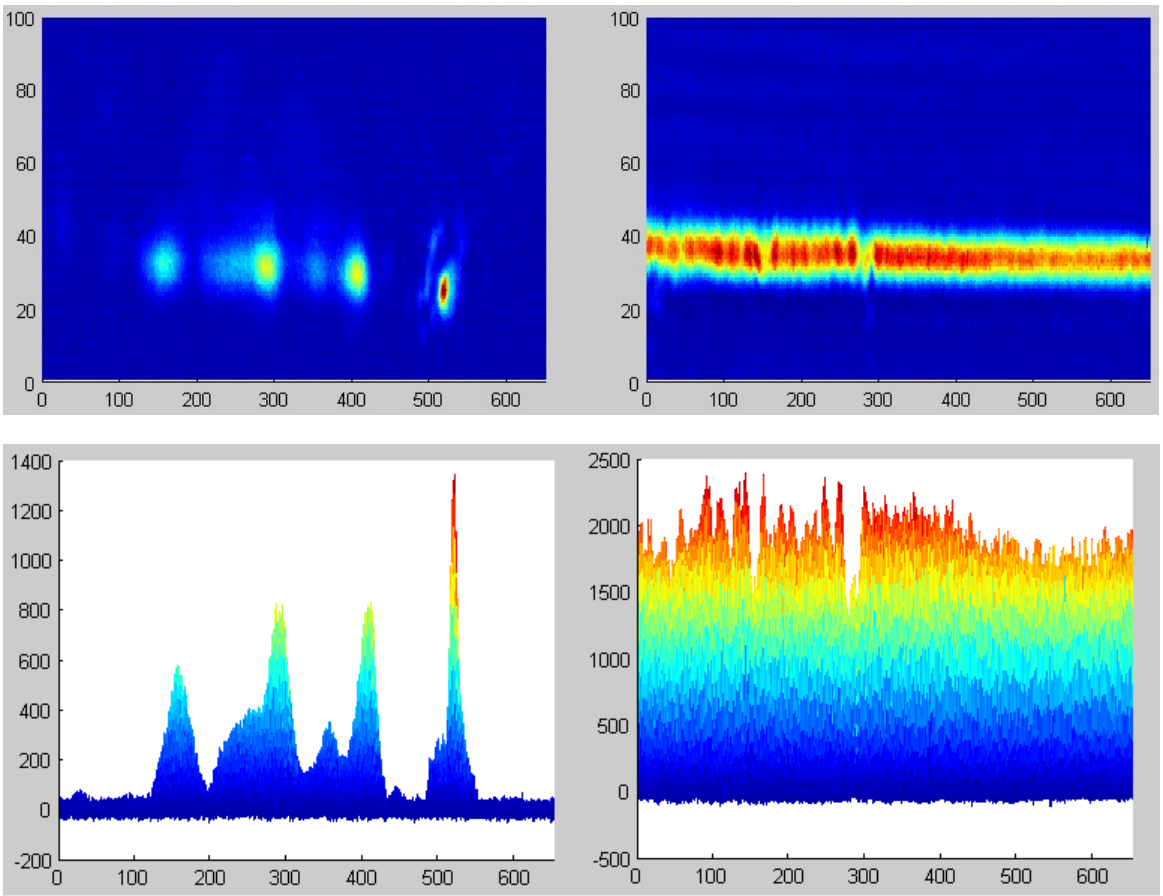

Figure 4. Top: near-field profile at the end-face of a 50 µm wide (left) and an "infinitely" wide waveguide (right). The axes represent camera pixels (1 pixel = ~110 nm) and the color scale represents intensity (arbitrary units). Bottom: cross-section of the near-field profile along the middle of the waveguide thickness, for both waveguides. The horizontal axis represents camera pixels and the vertical axis intensity (arbitrary units).

4.2 Demonstration of particle detection

In order to test the compatibility of the fabricated waveguides with the biosensing detection principle, LightLink rectangular waveguides were prepared and mounted in a setup, and the detection region was brought into contact with superparamagnetic 500 nm particles (prototype Dynabeads®) sourced from Life Technologies. In Figure 5, a schematic of the setup is shown.

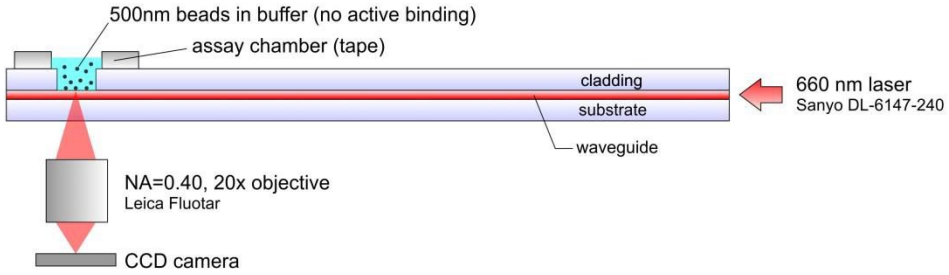

Figure 5. Schematic of the setup used to test the nanoparticle detection principle.

Waveguides were excited using butt-coupling of a 660 nm wavelength laser with a long working distance objective lens (NA = 0.4). The excited modes propagate along the waveguide and reach the detection area where the nanoparticles scatter light out of the evanescent field. The scattered light was collected by a 20x objective (NA = 0.4) and imaged with a CCD camera.

A fluid chamber was implemented in the detection region of the waveguide chamber. Thus, a liquid sample with particles could be deposited and subsequently monitored using dark field imaging. The monitoring was performed by detecting the scattered light from the particles that were present in the evanescent field extending into the liquid layer.

Wet and dried-in particles were tested with different intensities. Figure 6 illustrates examples of the bright field (bulk excitation) and dark field (waveguide excitation) images of the chamber visualized in the experiment.

From the detection experiments, we can conclude that single particles are excited by the waveguide evanescent field (Figure 6, right) and can be imaged with good signal-to-noise ratio. In addition, only low amounts of stray light can be observed in the transition between the propagating and detection regions. Hardly any light is scattered from particles at the region where the upper cladding is present. However, the non-uniformity of the waveguide modes intensity distribution causes a strong position dependence of the amount of scattered light. We expect to overcome this issue by using slab waveguides, allowing only one mode to propagate in the waveguide, resulting in a more homogeneous lateral intensity distribution.

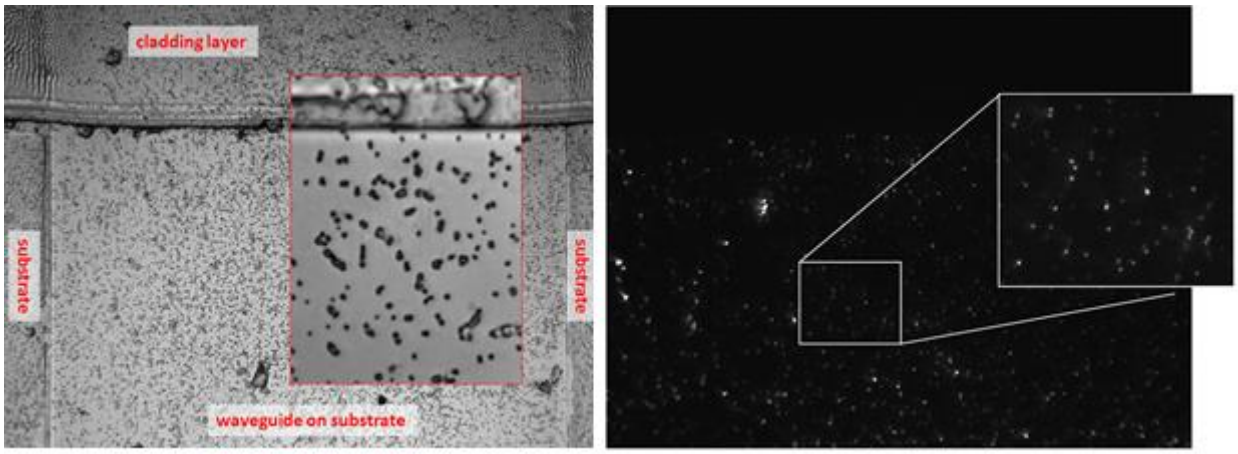

Figure 6. Left: Bright field microscope image of a waveguide covered with dried-in particles. Right: Dark field image of light from the waveguide evanescent field scattered by dried-in particles. The image was recorded with low laser power (<1mW).

5 CONCLUSIONS

Polymer waveguides have been designed and fabricated for the optical detection of nanoparticles in an evanescent field based biosensor. Penetration depth, evanescent field uniformity and polymer layer roughness were the main parameters considered to achieve an evanescent field capable of detecting single nanoparticles with good signal-to-noise ratio. Several polymer waveguide samples were fabricated using Ormocer, mr-LDW and LightLink materials and photolithographic patterning. Using these waveguides, the detection of single 500 nm dried-in particles was demonstrated.

ACKNOWLEDGEMENT

This work was conducted in the framework of the project NextDx, funded within the European Commission FP7 program.

REFERENCES

[1] Bruls, D. M., Evers, T. H., Kahlman, J. A. H., Van Lankvelt, P. J. W., Ovsyanko, M., Pelssers, E. G. M., Schleipen, J. J. H. B., de Theije, F. K., Verschuren, C. A., van der Wijk, T., van Zon, J. B. A., Dittmer, W. U., Immink, A. H. J., Nieuwenhuis, J. H. and Prins, M. W. J., "Rapid integrated biosensor for multiplexed immunoassays based on actuated magnetic nanoparticles," Lab on a Chip, 9(24), 3504-3510 (2009).
[2] Fan, X., White, I. M., Shopova, S. I., Zhu, H., Suter, J. D., and Sun, Y., "Sensitive optical biosensors for unlabeled targets: A review," analytica chimica acta, 620(1), 8-26 (2008).
[3] Sang, S., Zhang, W., and Zhao, Y., [State of the Art in Biosensors - General Aspects], InTech, Published Online, Chapter 4 (2013).
[4] Hoa, X. D., Kirk, A. G., and Tabrizian, M., "Towards integrated and sensitive surface plasmon resonance biosensors: a review of recent progress," Biosensors and Bioelectronics, 23(2), 151-160 (2007).
[5] Majewski, A., Sujecki, S., "Modes in rectangular fibers," Optoelectronics Review, 4 (1/2), 46-50 (1996).
[6] Hunsperger, R. G., [Integrated optics: theory and technology], Springer, New York, (2002).